Multiphoton processes and higher resonances in the quantum regime of the free-electron laser

Peter Kling [1,*] and Enno Giese [2]

[1]*German Aerospace Center (DLR), Institute of Quantum Technologies, Wilhelm-Runge-Straße 10, D-89081 Ulm, Germany*

[2]*Technische Universität Darmstadt, Fachbereich Physik, Institut für Angewandte Physik, Schlossgartenstr. 7, D-64289 Darmstadt, Germany*

(Received 29 March 2023; accepted 7 June 2023; published 27 July 2023)

Despite exhibiting novel radiation features, the operation of the proposed quantum free-electron laser would have the drawback that the number of emitted photons is limited by one per electron, significantly reducing the output power of such a device. We show that relying on different resonances of the initial momentum of the electrons increases the number of emitted photons, but also increases the required length of the undulator impeding an experimental realization. Moreover, we investigate how multiphoton processes influence the dynamics in the deep quantum regime.

DOI: 10.1103/PhysRevResearch.5.033057

I. INTRODUCTION

The quantum free-electron laser (Quantum FEL) [1–8] is a proposed radiation source which shows outstanding radiation features in the x-ray regime [9,10] and is anticipated to be a useful tool for applications in material and life sciences [11,12]. We focused in recent studies [5,10,13] on single-photon scattering to describe the dynamics of the system. In this paper, we complement these studies and show how multiphoton processes as well as different resonances of the initial electron momentum affect the FEL dynamics and we discuss their consequences for an experimental realization.

According to Ref. [14], the occurrence of higher-order resonances and the resulting dynamics would be absent in a semiclassical model. In contrast, we offer an elementary explanation for higher resonances in terms of energy-momentum conservation that is still captured by the semiclassical Hamiltonian.

The underlying mechanism of FEL physics is Compton scattering [15], where an electron absorbs a wiggler photon and emits a laser photon—or the vice versa process. Consequently, the momentum p of the electron changes by a discrete recoil $q \equiv 2\hbar k$, where $\hbar$ represents the reduced Planck constant and k is the wave number of the laser and as well of the wiggler field in the nearly comoving Bambini-Renieri frame [16,17].

During such an elastic scattering event not only the total momentum has to be conserved, but also the kinetic energy $\sim p^2$. From energy-momentum conservation we obtain (also higher-order) resonances for the initial momentum at integer multiples of $q/2$. The emergence of these resonances is visualized in Fig. 1 by identifying the resonant transitions with the help of energy parabolas in momentum space.

The first resonant process at $p = q/2$ occurs when the electron resonantly emits *one* laser photon and it jumps to the momentum $-q/2$. By the inverse process the electron can return to $q/2$ resulting in a two-level system, which we identified in Ref. [5] as Quantum FEL in accordance with Ref. [9]. In contrast, for $p = q$ there is no resonant single-photon transition. However, the electron can take two steps on the momentum ladder from q to $-q$ while emitting *two* laser photons.

At first sight, such higher resonances seem favorable since more emitted photons imply a higher output intensity. However, the typical timescale of the dynamics increases for higher resonances [8,14]. A longer interaction time requires a longer undulator and thus adds additional challenges to an experimental realization of a Quantum FEL [18]. Moreover, damping mechanisms like spontaneous emission [19] or space-charge effects [8,20,21] destroy an efficient Quantum FEL operation already for relatively small interaction times [11].

According to Fig. 1, the number of involved momentum steps and by that the number of emitted/absorbed photons increases for higher-order resonances. Probabilities for multiphoton processes scale in general with powers of the coupling strength between light and matter. Specifically, in the quantum theory of the FEL this behavior implies a scaling in powers of the quantum parameter, that is the ratio of the coupling strength to the recoil. For quantum effects to emerge, this parameter has to be small [5] and thus multiphoton transitions are suppressed when compared to the single-photon processes at $p = q/2$. In this paper we prove this behavior by employing the method of averaging over rapid oscillations [22,23] in the low-gain regime (Sec. II), where the change of the photon number is small compared to the number of photons already present, as well as in the high-gain regime (Sec. III) of FEL operation, where this assumption is dropped.

In Appendix A, we derive the effective Hamiltonian of our asymptotic method. While we deal in Appendix B with the population of the momentum levels in the low-gain regime, we show in Appendix C our calculations in the high-gain regime.

*Corresponding author: peter.kling@dlr.de

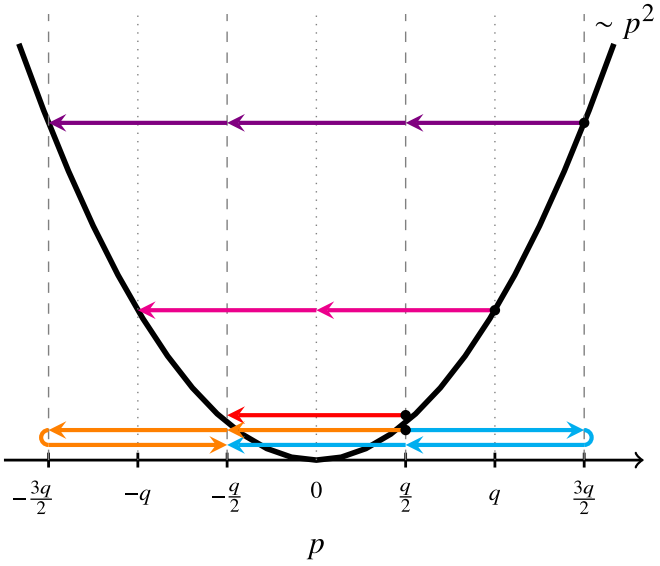

FIG. 1. Resonant transitions in an FEL visualized by energy-momentum conservation. We have drawn the kinetic energy $\sim p^2$ (parabola) of an electron as a function of the momentum p in the Bambini-Renieri frame [16], where the wave numbers of the laser and the wiggler mode coincide, that is $k \equiv k_{\mathrm{L}} = k_{\mathrm{W}}$ and the motion of the electron is nonrelativistic. In an elastic Compton-scattering event a wiggler photon is annihilated and a laser photon is emitted, or vice versa. Hence, (i) the momentum of the electron changes by multiples of the recoil $q \equiv 2\hbar k$ and (ii) the total kinetic energy of electron and photons has to be conserved. The first condition implies that the distance between initial and final momenta has to be an integer multiple of q. The second condition means that only transitions are allowed that horizontally connect two points on the energy parabola. (These points have the same distance from the x axis due to our specific frame of reference.) These two conditions are only fulfilled by initial and final momenta of the form $p = \nu q/2$ with ν being an integer. We consider single-, two-, and three-photon transitions from the three lowest resonant momenta, that is $p = q/2$, $p = q$, and $p = 3q/2$ to a different resonant momentum. For the first resonance, the transition from $q/2$ to $-q/2$ is resonant, which can be achieved by the emission of a single photon or via three-photon processes, where two photons are emitted and one photon is absorbed. Regarding the second resonance there are no resonant transitions with an odd number of photons. However, transitions with an even number of photons can be resonant, for example two-photon processes between q and $-q$. For the third resonance, we require at least three momentum steps to connect the momenta $3q/2$ and $-3q/2$. We note that the situation is mirrored for the momenta $-q/2$, $-q$, and $-3q/2$, with photon emission interchanged with absorption.

II. LOW-GAIN FEL

In the low-gain regime of FEL operation [24], the mean photon number $n \equiv \langle \hat{n} \rangle$ changes only marginally during the interaction with an electron bunch and the motion of an electron decouples from the motion of the others [25]. Hence, we restrict ourselves to the quantized motion of a single electron with mass m coupled to a classical and fixed radiation field.

Our model relies on the Bambini-Renieri [16] frame of reference which is defined by the condition that the given wave number $k_{\mathrm{W}} \equiv 2\pi/\lambda_{\mathrm{W}}$ of the (optical) undulator and the desired wave number $k_{\mathrm{L}} \equiv 2\pi/\lambda_{\mathrm{L}}$ of the laser field coincide after performing a Lorentz transformation into the moving frame, that is $k_{\mathrm{L}}, k_{\mathrm{W}} \to k$. From this requirement, we find [5] that the Bambini-Renieri frame moves at the velocity

$$\frac{v_{\mathrm{BR}}}{c} \equiv \frac{k_{\mathrm{L}} - k_{\mathrm{W}}}{k_{\mathrm{L}} + k_{\mathrm{W}}} \tag{1}$$

relative to the laboratory frame. For the relevant case, where $\lambda_{\mathrm{L}} \ll \lambda_{\mathrm{W}}$, we obtain that the Lorentz factor $\gamma_{\mathrm{BR}} \equiv (1 - v_{\mathrm{BR}}^2/c^2)^{-1/2}$ corresponds to a relativistic motion, that is $\gamma_{\mathrm{BR}} \gg 1$. The advantages of choosing this special reference frame are that (i) the dynamics is described by the motion of a particle in a standing wave and (ii) that this motion is non-relativistic, if the transformed momentum of the electron is much smaller than mc. In the quantum regime the typical momentum scale is given by the recoil $q \equiv 2\hbar k$ and we indeed observe that $q/(mc) \approx \lambda_{\mathrm{C}}/(\gamma_{\mathrm{BR}}\lambda_{\mathrm{L}}) \ll 1$ since the Compton wavelength $\lambda_{\mathrm{C}} \sim 10^{-12}$ m of the electron is much smaller than any realistic laser wavelength [5]. Hence, the Bambini-Renieri frame is—almost—comoving with the electron.

The motion of an electron with initial momentum p may only change by integer multiples of the recoil q. We describe the resulting momentum ladder through the momentum jump operator

$$\hat{\sigma}_{\mu,\nu} \equiv |p - \mu q\rangle \langle p - \nu q| \tag{2}$$

with μ and ν being integers.

In Ref. [5], we defined the quantum parameter $\alpha_n \equiv g\sqrt{n}/\omega_{\mathrm{r}}$ as the ratio of the coupling strength $g\sqrt{n}$, depending on the mean photon number n, and the recoil frequency $\omega_{\mathrm{r}} \equiv q^2/(2m\hbar)$. The coupling constant g is proportional to the undulator parameter a_0, that is the normalized field strength of the wiggler [18]. For quantum effects to emerge, we require (i) that the quantum parameter is small, that is $\alpha_n \ll 1$, and (ii) that the initial momentum spread Δp of the electron beam is small, that is $\Delta p \ll q$. Else, the discrete motion of the electron is washed out and the particle follows continuous trajectories [5,26]. Throughout this paper, we assume for simplicity that the electron is initially described by a momentum eigenstate $|p\rangle$. In a more realistic model, the state of the electron should be described by a momentum distribution with a nonzero width Δp [27]. Due to velocity selectivity, the efficient operation of a Quantum FEL is only possible, if Δp is smaller than the gain bandwidth $\sim\alpha_n q$ [13]. According to Ref. [11] a possible design for a Quantum FEL in the ångström-regime could include a high-power optical undulator with a wavelength λ_W in the micrometer range and a high-quality electron beam with a relative energy spread at the order of 10^{-5}.

The asymptotic method of averaging separates the resonant processes from the nonresonant ones. For the former ones, we formulate an effective Hamiltonian $\hat{H}_{\mathrm{eff}}$ [23] and asymptotically expand it in powers of α_n. We solve the resulting Schrödinger equation exactly, which gives rise to slowly varying part of the dynamics. For the nonresonant transitions, we rely on a perturbative solution which leads to amplitude corrections including rapidly varying terms. Each additional step on the momentum ladder raises the order of the asymptotic expansion by one.

In the following, we consider the change of the mean photon number $\delta n_p(t) \equiv \langle \hat{n}(t) \rangle - \langle \hat{n}(0) \rangle$ during the interaction

of an electron bunch containing N electrons of momentum p with the fields. In the low-gain regime, this change has to be smaller than the initial photon number $n_0 \equiv \langle \hat{n}(0) \rangle$, that is $\delta n_p \ll n_0$. Since each momentum step translates to the emission or absorption of a photon, we calculate the change δn_p via the relation

$$\delta n_p(t) = N \sum_{\mu} \mu \, P_{p-\mu q}(t), \tag{3}$$

where $P_{p-\mu q}$ denotes the time-dependent probability that the momentum level $p - \mu q$ is populated.

According to Appendix B, we find that for the initial condition $p = \nu q/2$, the population of levels $\pm \nu q/2$ corresponding to resonant transitions are described by Rabi oscillations between zero and unity, while the probabilities corresponding to nonresonant transitions are suppressed with powers of α_n. With the help of the explicit expressions for the $P_{p-\mu q}$ in Appendix B we arrive at the results

$$\delta n_{q/2}(t) \cong N \sin^2 \left[\Omega t \left(1 - \frac{\alpha_n^2}{4} \right) \right], \tag{4a}$$

$$\delta n_q(t) \cong 2N \sin^2 \left[\alpha_n \Omega t \left(1 - \frac{16\alpha_n^2}{9} \right) \right], \quad \text{and} \tag{4b}$$

$$\delta n_{3q/2}(t) \cong 3N \sin^2 \left(\frac{\alpha_n^2}{4} \Omega t \right) \tag{4c}$$

of δn_p for the first, second, and third resonance, where we have defined the Rabi frequency $\Omega \equiv g\sqrt{n}$ of the fundamental resonance $q/2$. Here we have only included the leading orders in amplitude and the lowest-order corrections in frequency. We obtain that for higher resonances (i) the number of maximally emitted photons increases, but also that (ii) the effective Rabi frequency becomes smaller leading to a slower growth of the mean photon number as apparent from Fig. 2.

The calculation of higher-order resonances requires higher orders of the asymptotic expansion and consequently this increase of time scales continues beyond the third resonance. Hence, we expect the scaling

$$\Omega^{(\nu)} \propto \alpha_n^{\nu-1} \Omega \tag{5}$$

for the effective Rabi frequency $\Omega^{(\nu)}$ that corresponds to the resonant transition from $\nu q/2$ to $-\nu q/2$ [25]. We emphasize that the emergence of different time scales for different initial momenta follows directly from the number of momentum steps necessary for a resonant transition. An analogous behavior has been also observed in atomic diffraction [28,29]. However, since we observe this dynamics in a semiclassical model, it has nothing to do with a quantized light field in contrast to the assumption of Ref. [14].

III. HIGH-GAIN FEL

In the high-gain regime of FEL operation, the relative change of the laser intensity during the interaction with the electrons is large and consequently the laser field cannot be seen as an fixed, external field. In contrast, the motion of each electron in the bunch influences the motion of the remaining electrons via their common interaction with the laser field [13,30].

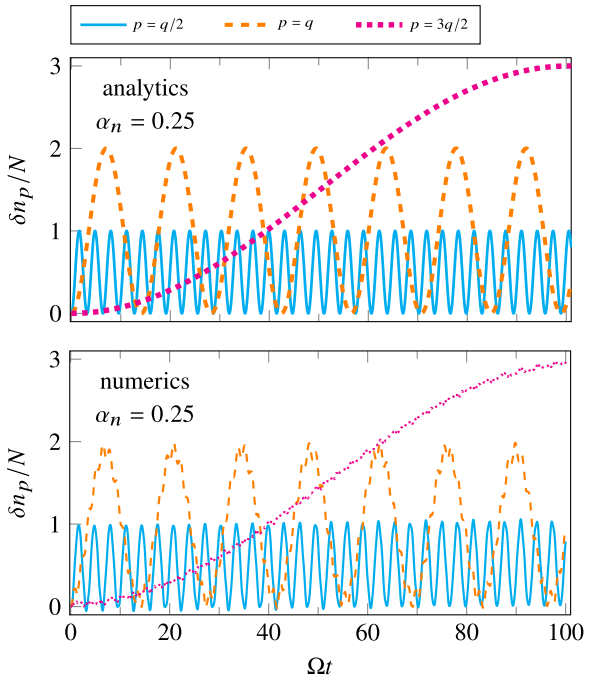

FIG. 2. Change δn_p of the mean photon number in a low-gain FEL in the quantum regime divided by the number N of electrons as a function of the phase Ωt with the Rabi frequency Ω for the first resonance at $p = q/2$. We compare the curves for three different initial electron momenta, that is (i) $p = q/2$ (cyan line), (ii) $p = q$ (orange, dashed line), and (iii) $p = 3q/2$ (magenta, dotted line) for a fixed value of the quantum parameter of $\alpha_n = 0.25$. If we increase the order of the resonance, the number of emitted photons per electron increases. However, the photon number grows more slowly for higher resonances. We observe that the analytical results (top) from Eq. (4) and the numerical simulation (bottom) agree.

In analogy to Ref. [13], we employ a collective model, where the single-particle jump operators are replaced by their collective counterparts, that is,

$$\hat{\sigma}_{\mu,\nu} \to \hat{\Upsilon}_{\mu,\nu} \equiv \sum_{j=1}^{N} \hat{\sigma}_{\mu,\nu}^{(j)}, \tag{6}$$

where $\hat{\sigma}_{\mu,\nu}^{(j)}$ is the single-particle operator for electron j. We assume that each electron is initially described by a momentum eigenstate with the same momentum p yielding the product state $|p, p, \ldots, p\rangle$. Moreover, we introduce a quantized laser mode with bosonic annihilation and creation operators satisfying the commutation relation $[\hat{a}_{\mathrm{L}}, \hat{a}_{\mathrm{L}}^{\dagger}] = 1$. For the calculation of the mean photon number we restrict ourselves to an FEL seeded by a Fock state with n_0 photons. In Ref. [10], we observed that the results for the mean photon number of a Quantum FEL are very similar for other initial field states with the same n_0, such as coherent or thermal states.

In Refs. [10,13], we found that the leading order of the effective Hamiltonian for the first resonance $p = q/2$ is given by the Dicke Hamiltonian, which describes the collective interaction of many two-level atoms with a quantized mode of the radiation field [31].

In the current paper, we include the lowest-order corrections emerging from the higher orders of $\hat{H}_{\mathrm{eff}}$ derived

in Appendix A. From the results in Ref. [10] and from Eqs. (C8) and (C10a), we deduce for $p = q/2$ the approximate expression

$$n_{q/2}(L) = n_0 + N\mathrm{cn}^2\left[\sqrt{1+\frac{n_0}{N}}\frac{L}{2L_g}\left[1-\frac{\alpha_N^2}{8}\left(1+\frac{2n_0}{N}\right)\right]-K,\,\mathfrak{K}\right] \tag{7}$$

for the mean photon number $n_{q/2}$ as a function of the undulator length $L \equiv ct$. Here c denotes the velocity of light and $L_g \equiv c/(2g\sqrt{N})$ represents the gain length of a Quantum FEL [9,13]. The Jacobi elliptic function cn depends on its modulus $\mathfrak{K} \equiv (1+n_0/N)^{-1/2}$ and $K \equiv K(\mathfrak{K})$ denotes the corresponding complete elliptic integral of first kind [32]. We note that the quantum parameter $\alpha_N \equiv g\sqrt{N}/\omega_\mathrm{r}$ for the high-gain regime depends on the number N of electrons in the bunch. For simplicity, we have neglected in Eq. (7) the terms responsible for spontaneous emission when compared to the result in Ref. [10]. Accordingly, the expression for $n_{q/2}$ goes to zero for $n_0 = 0$.

In the top panel of Fig. 3, we compare the approximation for n to the numerical simulation corresponding to the effective Hamiltonian up to third order. For $\alpha_N \ll 2\sqrt{2}$, the phase corrections in Eq. (7) are negligible and thus we obtain only a small phase shift for $\alpha_N = 0.5$ between third-order and first-order results of the asymptotic method of averaging. While this frequency shift is perfectly predicted by Eq. (7), numerics reveals a very small suppression of the amplitude which arises from resonant second-order processes, where one photon is emitted and another one is absorbed.

For the second resonance $p = q$, we observe that the effective Hamiltonian is analogous to a two-photon Dicke Hamiltonian [33,34]

$$\hat{H}_{2\mathrm{ph}} = \frac{\alpha_N^2}{N}\left(\hat{a}_\mathrm{L}^2\hat{\Upsilon}_{0,2} + \hat{a}_\mathrm{L}^{\dagger 2}\hat{\Upsilon}_{2,0}\right) \tag{8}$$

describing the transitions between the levels q and $-q$ (compare to Appendix A). Moreover, we find a second contribution to this effective Hamiltonian that includes two-photon transitions, where one photon is emitted and one is absorbed in rough analogy to the origin of the Stark shift.

To derive an approximate solution for the second resonance, we restrict ourselves for simplicity to the contribution corresponding to the two-photon Dicke Hamiltonian. In analogy to Refs. [10,35], we employ two constants of motion to find in Appendix C the expression

$$n_q(L) = n_0\frac{1+\frac{n_0}{2N}}{\cos^2\left[\sqrt{\frac{n_0}{N}\left(\frac{n_0}{N}+2\right)}\frac{\alpha_N L}{2L_g}\right]+\frac{n_0}{2N}} \tag{9}$$

for the mean photon number within a semiclassical approximation that neglects terms responsible for spontaneous emission.[1] Moreover, we compute in Appendix C a numerical solution in rough analogy to the procedure for the fundamental resonance [36].

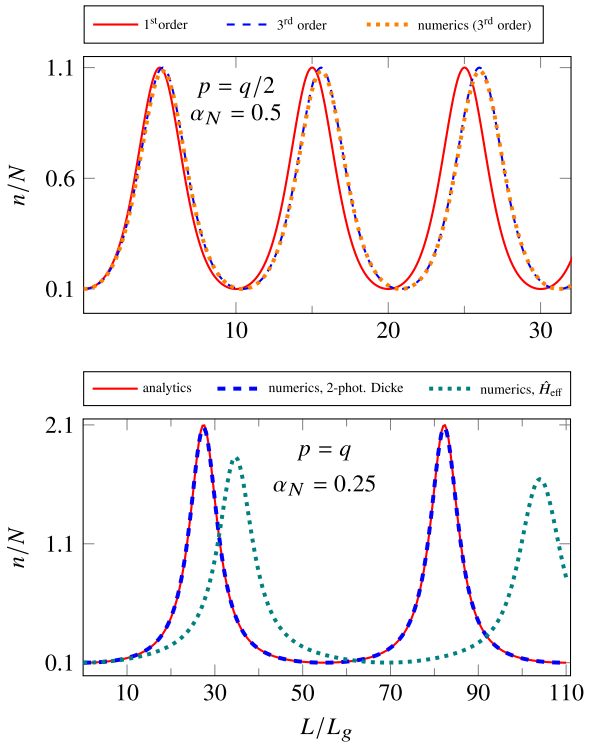

FIG. 3. Mean photon number n of a seeded high-gain FEL in the quantum regime divided by the number N of electrons as a function of the undulator length L in units of the gain length L_g. The initial photon number amounts to $n_0 = 0.1N$ and the electron number to $N = 10^4$. In the top panel all electrons start at the first resonance $p = q/2$. We observe that the analytical solution (blue, dashed line) from Eq. (7) including third-order corrections agrees with the numerical solution corresponding to the effective Hamiltonian in third order (orange, dotted line), while the first-order solution (red line) of Ref. [10] differs by a phase shift $\sim\alpha_N^2$. We have chosen the comparably high value $\alpha_N = 0.5$ for the quantum parameter to make this shift visible. In the bottom panel all electrons start at the second resonant momentum $p = q$ with $\alpha_N = 0.25$. Here we compare the analytical approximation (red line) from Eq. (9) to the numerical simulations resulting (i) from the two-photon Dicke Hamiltonian (blue, dashed line), and (ii) from the full effective Hamiltonian (green, dotted line) of second order. In all three cases we observe an oscillatory behavior, with at most two emitted photons per electron. Analytics and numerics agree for the simplified model, that is the two-photon Dicke Hamiltonian. However, the simulation for the full dynamics shows a suppressed maximum photon number which occurs after a higher interaction length in comparison to the curves corresponding to the simplified model. Nevertheless, the qualitative behavior is similar.

In the bottom panel of Fig. 3, we have drawn the mean photon number for $p = q$ as a function of the undulator length L. We observe that n_q shows an oscillatory behavior, with at most two emitted photons per electron. Compared to the solutions corresponding to the simplified model with the two-photon Dicke Hamiltonian, the curve emerging from the simulation of the full effective Hamiltonian of second order has a suppressed maximum which occurs after a slightly higher interaction length.

[1] For a small interaction length L, we find the asymptotic behavior $n \cong n_0[1 + n_0(\alpha_N L/L_g)^2/(2N)]$. Hence, a linear analysis (often used in FEL theory) is not sufficient to obtain this nonlinear short-time behavior.

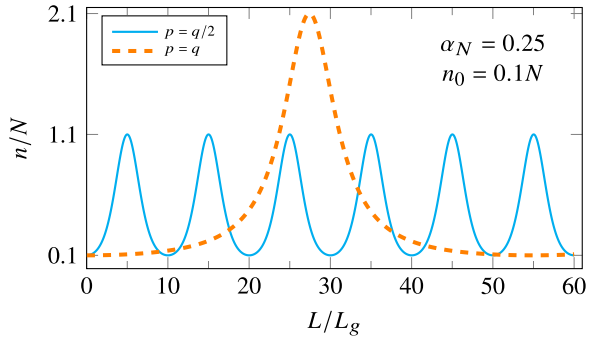

FIG. 4. Mean photon number n of a seeded high-gain FEL in the quantum regime divided by the number N of electrons as a function of the undulator length L in units of the gain length L_g. We compare the curves corresponding to the two analytical expressions Eqs. (7) and (9), where the electrons start at (i) the first resonant momentum $p = q/2$ (blue line) and (ii) the second resonance $p = q$ (orange, dashed line). We have chosen the values $n_0 = 0.1N$ and $\alpha_N = 0.25$ for the initial photon number and the quantum parameter, respectively. The second resonance leads to maximally two emitted photons per electron compared to only one for the first resonance. However, for $p = q$, the growth of the photon number is much slower and the maximum occurs at a much higher interaction length compared to $p = q/2$. Hence, we deduce that the first resonance is more advantageous for the realization of a high-gain Quantum FEL than higher resonances.

Similar to the low-gain regime, the maximum photon number increases for higher resonances, but at the same time the growth of the photon number becomes slower. We identify this effect directly in the analytical results. For the second resonance, the maximum photon number $n^q_{\max} = n_0 + 2N$ occurs at the length $L^q_{\max}$ while the corresponding maximum $n^{q/2}_{\max} = n_0 + N$ for $p = q/2$ is reached at $L^{q/2}_{\max}$. With the help of Eqs. (7) and (9), we obtain the relation

$$\frac{L^q_{\max}}{L^{q/2}_{\max}} = \frac{1}{\alpha_N} \frac{\pi}{2\ln\left(\sqrt{\frac{N}{n_0}}\right)\sqrt{\frac{n_0}{N}\left(\frac{n_0}{N}+2\right)}}. \tag{10}$$

Due to the scaling with $1/\alpha_N \gg 1$, the maximum for $p = q$ is shifted to the right compared to $p = q/2$. We visualize this behavior in Fig. 4, where we have drawn the mean photon numbers corresponding to these two resonances both as functions of the undulator length. We derive from Eq. (10) with $n_0 = 0.1N$ that $L^q_{\max} \lesssim L^{q/2}_{\max}$ only for $\alpha_N \gtrsim 3$ which is outside the quantum regime for which we require a small value of α_N.

The results in the high-gain regime, Eqs. (7) and (9), reduce to their respective low-gain counterparts in Eq. (4) in the asymptotic limit $\delta n \sim N \ll n_0$. Moreover, we emphasize that the quantum regime as well as the classical regime are both opposite asymptotic limits of the quantum theory of the FEL. The transition between classical an quantum is for example discussed in Ref. [26] for the low-gain or in Ref. [9] for the high-gain regime.

IV. CONCLUSIONS

The quantum regime of the FEL emerges for high values of the quantum mechanical recoil, that is small wavelengths. Optical undulators are key [3,37] to achieve such parameters experimentally. The requirements on power and pulse length of such a "pump laser" [18] pose hard experimental challenges, already for the lowest-order [10] momentum resonance $p = q/2$. In addition, the combined influence of space charge and spontaneous emission limits the maximally possible interaction length [11]. In this paper we demonstrated that higher-order resonant transitions require even larger undulator lengths due to the suppression of multiphoton transitions in the quantum regime. As a consequence, the first resonance is favorable compared to the higher-order ones.

Moreover, we calculated multiphoton corrections to the deep quantum regime at $p = q/2$ in the low-gain [5] and for the first time also in the high-gain regime. Besides multiphoton processes, space charge and spontaneous emission can destroy the Quantum FEL dynamics [11]. Only recently [8], space-charge effects were studied in detail in a semiclassical phase-space model. In the next steps, one could combine all mentioned effects in a more complete Quantum FEL theory to specify more accurately parameter regimes, where an experimental realization becomes possible.

ACKNOWLEDGMENTS

We thank W. P. Schleich, R. Sauerbrey, C. M. Carmesin, A. Debus, and K. Steiniger for many exciting discussions.

APPENDIX A: EFFECTIVE HAMILTONIAN

We start with the dimensionless Hamiltonian in the high-gain regime [13]

$$\hat{H} \equiv \varepsilon \sum_{\mu} (e^{i2\tau[\frac{p}{q}-(\mu+\frac{1}{2})]}\, \hat{a}_{\mathrm{L}} \hat{\Upsilon}_{\mu,\mu+1} + \text{H.c.}) \tag{A1}$$

in the interaction picture with the dimensionless coupling constant $\varepsilon \equiv g/\omega_{\mathrm{r}}$ and the dimensionless time variable $\tau \equiv \omega_{\mathrm{r}} t$. To obtain the single-electron and semiclassical Hamiltonian for a low-gain FEL, we simply have to replace the collective operators $\hat{\Upsilon}_{\mu,\nu}$ by their single-particle counterparts $\hat{\sigma}_{\mu,\nu}$ and approximate $\hat{a}_{\mathrm{L}} \approx \hat{a}^{\dagger}_{\mathrm{L}} \approx \sqrt{n} \approx \text{const}$. This approximation is only valid, if the relative change $\delta n/n$ of the mean photon number is much smaller than unity. We deduce from Fig. 1 that in the quantum regime an electron at the νth resonance $p = \nu q/2$ emits at most ν photons leading to condition $\nu N/n \ll 1$ for being in the low-gain regime. We note that the commutation relation

$$[\hat{\Upsilon}_{\mu,\nu}, \hat{\Upsilon}_{\rho,\sigma}] = \delta_{\nu,\rho} \hat{\Upsilon}_{\mu,\sigma} - \delta_{\sigma,\mu} \hat{\Upsilon}_{\rho,\nu} \tag{A2}$$

for the jump operators is the same for the collective model as in the single-electron limit. However, the properties of products of these operators differ [13].

The asymptotic method of averaging [22,23,25] is suitable for a Hamiltonian $\hat{H}$ which can be represented as a Fourier series in terms of the phase τ and its integer multiples. We separate slow and rapid dynamics in the state vector $|\Psi(\tau)\rangle \equiv \exp[-\hat{F}(\tau)]\,|\Phi(\tau)\rangle$, where $\hat{F}$ describes the rapidly varying part, while $|\Phi\rangle$ gives the slowly varying part. With the help

TABLE I. Effective Hamiltonian: We present for different resonant momenta the contributions of the asymptotic expansion of $\hat{H}_{\rm eff}$ in orders of α_n in the low-gain regime and in orders of ε in the high-gain regime, respectively. For the first and the second resonance, $p = q/2$ and $p = q$, we give the effective Hamiltonian up to third order. Moreover, we have calculated the fourth-order contribution in the case of $p = q$. For the third resonance $p = 3q/2$, we have restricted ourselves to the low-gain regime.

	Low gain: $\hat{H}_{\rm eff} \cong$	High gain: $\hat{H}_{\rm eff} \cong$
$p = \frac{q}{2}$	$\alpha_n[\hat{\sigma}_{1,0} + \hat{\sigma}_{0,1}]$ $+\alpha_n^2\left[-\frac{1}{2}(\hat{\sigma}_{0,0} + \hat{\sigma}_{1,1}) + \sum_{\mu\neq 0,1} \frac{\hat{\sigma}_{\mu,\mu}}{2\mu(\mu-1)}\right]$ $-\frac{\alpha_n^3}{4}[\hat{\sigma}_{0,1} + \hat{\sigma}_{1,0} - \hat{\sigma}_{-1,2} - \hat{\sigma}_{2,-1}]$	$\varepsilon[\hat{a}_{\rm L}\hat{\Upsilon}_{1,0} + \hat{a}_{\rm L}^\dagger\hat{\Upsilon}_{0,1}]$ $+\frac{\varepsilon^2}{2}\left[(\hat{n}+1)\sum_{\mu\neq 0}\frac{1}{\mu}(\hat{\Upsilon}_{\mu+1,\mu+1} - \hat{\Upsilon}_{\mu,\mu}) - \sum_{\mu\neq 0}\frac{1}{\mu}\hat{\Upsilon}_{\mu+1,\mu}\hat{\Upsilon}_{\mu,\mu+1}\right]$ $+\frac{\varepsilon^3}{4}\left[\hat{a}_{\rm L}\sum_{\mu\neq -1,0}\frac{\hat{\Upsilon}_{2\mu+2,2\mu+1}\hat{\Upsilon}_{\mu,\mu+2}}{\mu(\mu+1)(2\mu+1)} + \frac{3\hat{a}_{\rm L}}{2}(\hat{\Upsilon}_{0,-1}\hat{\Upsilon}_{-1,1} - \hat{\Upsilon}_{0,2}\hat{\Upsilon}_{2,1})\right.$ $\left.-\left(\sum_{\mu\neq 0}\frac{\hat{\Upsilon}_{\mu+1,\mu+1}-\hat{\Upsilon}_{\mu,\mu}}{2\mu^2} + \hat{n} + \frac{1}{2}\right)\hat{a}_{\rm L}\hat{\Upsilon}_{0,1} + \hat{a}_{\rm L}^3\hat{\Upsilon}_{-1,2} + \text{H.c.}\right]$
$p = q$	$\alpha_n^2\left[\hat{\sigma}_{0,2} + \hat{\sigma}_{2,0} + \sum_\mu \frac{2\hat{\sigma}_{\mu,\mu}}{(2\mu-3)(2\mu-1)}\right]$ $+\alpha_n^4\left[-\frac{16}{9}(\hat{\sigma}_{2,0} + \hat{\sigma}_{0,2}) + \frac{1}{36}(\hat{\sigma}_{3,-1} + \hat{\sigma}_{-1,3})\right.$ $\left.-\sum_\mu \frac{\hat{\sigma}_{\mu+1,\mu+1}-\hat{\sigma}_{\mu,\mu}}{8(\mu-1/2)^3\{(\mu-1/2)^2-1\}^2} + \sum_{\mu\neq 0}\frac{\hat{\sigma}_{\mu+1,\mu+1}+\hat{\sigma}_{\mu,\mu}}{64\mu(\mu^2-1/4)^2}\right]$	$\varepsilon^2\left[\hat{a}_{\rm L}{}^2\hat{\Upsilon}_{0,2} + \text{H.c.} + \hat{n}\sum_\mu\frac{\hat{\Upsilon}_{\mu+1,\mu+1}}{2\mu-1} - (\hat{n}+1)\sum_\mu\frac{\hat{\Upsilon}_{\mu,\mu}}{2\mu-1}\right.$ $\left.+\sum_\mu\frac{\hat{\Upsilon}_{\mu+1,\mu+1}+\hat{\Upsilon}_{\mu,\mu}-\hat{\Upsilon}_{\mu+1,\mu}\hat{\Upsilon}_{\mu,\mu+1}-\hat{\Upsilon}_{\mu,\mu+1}\hat{\Upsilon}_{\mu+1,\mu}}{4\mu-2}\right]$
$p = \frac{3q}{2}$	$\alpha_n[\hat{\sigma}_{1,2} + \hat{\sigma}_{2,1}]$ $+\alpha_n^2\left[-\frac{1}{2}(\hat{\sigma}_{1,1} + \hat{\sigma}_{2,2}) + \sum_{\mu\neq 1,2}\frac{\hat{\sigma}_{\mu,\mu}}{2(\mu-1)(\mu-2)}\right]$ $+\frac{\alpha_n^3}{4}[\hat{\sigma}_{0,3} + \hat{\sigma}_{3,0} - \hat{\sigma}_{1,2} - \hat{\sigma}_{2,1}]$	

of this ansatz, we derive the effective Hamiltonian [23]

$$\hat{H}_{\rm eff} = \sum_{j=0}^{\infty}\frac{1}{(j+1)!}\left[\hat{F}, i\frac{d\hat{F}}{d\tau}\right]_j + \sum_{j=0}^{\infty}\frac{1}{j!}[\hat{F},\hat{H}]_j \qquad \text{(A3)}$$

of the Schrödinger equation for $|\Phi\rangle$, where the subscript j indicates a j times nested commutator.

We proceed by asymptotically expanding $\hat{H}_{\rm eff}$ and $\hat{F}$ in powers of α_n, or in powers of ε in the high-gain regime. In each order of this expansion we have to ensure that the effective Hamiltonian is independent of time, that is $\hat{H}_{\rm eff} \neq \hat{H}_{\rm eff}(\tau)$. Hereby, we avoid secular contributions which otherwise lead to unphysically growing terms [38]. The dynamics dictated by $\hat{H}_{\rm eff}$ can then be solved nonperturbatively. In contrast, we can rely on perturbation theory for the rapidly varying dynamics since here the secular terms are excluded by construction.

Depending on the specific initial momentum $p = \nu q/2$ with integer ν, we obtain from Eq. (A1) the explicit expressions for the Fourier components of $\hat{H}$. By inserting these components into $\hat{H}_{\rm eff}$ from Eq. (A3) and calculating the occurring commutators we finally obtain the effective Hamiltonian for low and high gain and for different resonances. We have listed the explicit expressions in Table I.

APPENDIX B: POPULATION OF MOMENTUM LEVELS

In this Appendix, we discuss the population probabilities of the momentum levels for an electron in a low-gain FEL resulting from the asymptotic method of averaging. For the first resonance $p = q/2$, we refer to Ref. [5], where the population probabilities for the momentum levels are listed up to third order in α_n for the frequency and up to second order for the amplitude. In the following, we consider the second and the third resonance.

1. Second resonance

The initial state of an electron for the second resonance is given by the momentum eigenstate $|\Psi(0)\rangle = |p\rangle$ with $p = q$. However, due to the transformation from $|\Psi\rangle$ to $|\Phi\rangle$ we calculate the transformed initial state $|\Phi(0)\rangle = \exp[\hat{F}(0)]\,|\Psi(0)\rangle$ perturbatively up to second order of α_n.

We expand the state $|\Phi\rangle$ in the discretized momentum basis with probability amplitudes $\langle p - \mu q|\Phi(\tau)\rangle$. The Schrödinger equation corresponding to the effective Hamiltonian from Table I then translates to a system of linear differential equations which we easily solve with respect to the initial conditions for $|\Phi\rangle$.

Then, we transform the result for $|\Phi\rangle$ back to the original state $|\Psi\rangle$ via the relation $|\Psi(\tau)\rangle = \exp[-\hat{F}(\tau)]\,|\Phi(\tau)\rangle$, and again restrict ourselves to terms up to second order of α_n. Finally, we calculate the probabilities $P_{p-\mu q}(\tau) \equiv |\langle p - \mu q|\Psi(\tau)\rangle|^2$ for the population of the momentum levels up to the order α_n^2 in amplitude and α_n^4 in frequency.

By this procedure, we find the explicit expressions

$$P_{2q}(\tau) = \frac{\alpha_n^2}{9}(\cos^2\xi_1\tau + \cos^2\xi_2\tau - 2\cos\xi_1\tau\cos\xi_2\tau\cos\xi_3\tau),$$

$$P_q(\tau) = \cos^2\xi_1\tau + 2\alpha_n^2\cos\xi_1\tau \times\left(-\frac{10}{9}\cos\xi_1\tau + \cos\xi_4\tau + \frac{1}{9}\cos\xi_2\tau\cos\xi_3\tau\right),$$

$$P_0(\tau) = 2\alpha_n^2\{1-\cos[(\xi_1+\xi_4)\tau]\},$$

$$P_{-q}(\tau) = \sin^2\xi_1\tau + 2\alpha_n^2\sin\xi_1\tau \times\left(-\frac{10}{9}\sin\xi_1\tau - \sin\xi_4\tau + \frac{1}{9}\sin\xi_2\tau\cos\xi_3\tau\right),$$

$$P_{-2q}(\tau) = \frac{\alpha_n^2}{9}(\sin^2\xi_1\tau + \sin^2\xi_2\tau - 2\sin\xi_1\tau\sin\xi_2\tau\cos\xi_3\tau),$$

with

$$\xi_1 \equiv \alpha_n^2\left(1-\frac{16\alpha_n^2}{9}\right),$$

$$\xi_2 \equiv \frac{\alpha_n^4}{36}\sqrt{1+\left(\frac{124}{125}\right)^2},$$

$$\xi_3 \equiv 3-\frac{8\alpha_n^2}{15}\left(1-\frac{16\alpha_n^2}{5}\right),$$

$$\xi_4 \equiv 1+\frac{8\alpha_n^2}{3}\left(1-7\left(\frac{8\alpha_n}{15}\right)^2\right).$$

We note that the sum over these probabilities equals unity.

2. Third resonance

For the third resonance, $p = 3q/2$, we neglect the amplitude corrections and assume that $|\Psi\rangle \approx |\Phi\rangle$. With the help of the effective Hamiltonian in Table I, we obtain the probabilities

$$P_{3q/2}(\tau) = \cos^2\left(\frac{\alpha_n^3\tau}{4}\right) \text{ and } P_{-3q/2}(\tau) = \sin^2\left(\frac{\alpha_n^3\tau}{4}\right) \tag{B1}$$

for the population of the momentum levels $3q/2$ and $-3q/2$, respectively.

APPENDIX C: CALCULATIONS IN HIGH-GAIN REGIME

We calculate the time evolution of the mean photon number for a high-gain FEL in the quantum regime at the second resonance. For that we employ (i) an analytical approximation and (ii) a numerical simulation.

1. Analytical approximation

The momentum jump operators appearing in the two-photon Dicke Hamiltonian $\hat{H}_{2\mathrm{ph}}$ from Eq. (8) can be treated analogously to ladder operators of angular momenta. For simplicity, we employ the Schwinger representation of angular momentum [39] by introducing the bosonic annihilation and creation operators, $\hat{b}_s$ and $\hat{b}_s^\dagger$, respectively for two modes $s = 0, 2$. We then identify the relations $\hat{\Upsilon}_{0,2} \equiv \hat{b}_0^\dagger\hat{b}_2$ and $\hat{\Upsilon}_{2,0} \equiv \hat{b}_2^\dagger\hat{b}_0$. Hence, we obtain the Hamiltonian

$$\hat{H}_{2\mathrm{ph}} = \varepsilon^2(\hat{a}_\mathrm{L}{}^2\hat{b}_0^\dagger\hat{b}_2 + \hat{a}_\mathrm{L}^{\dagger 2}\hat{b}_2^\dagger\hat{b}_0) \tag{C1}$$

from which we derive via the Heisenberg equations of motion the two constants of motion $\hat{A} \equiv \hat{N}_0 + \hat{N}_2 = \text{const}$, and $\hat{B} \equiv 2\hat{N}_0 + \hat{n} = \text{const}$ with $\hat{N}_k \equiv \hat{b}_k^\dagger\hat{b}_k$ and $\hat{n} \equiv \hat{a}_\mathrm{L}^\dagger\hat{a}_\mathrm{L}$ [35].

In the following, we approximate the operators as classical but dynamically changing variables. The Hamiltonian equation of motion for a dynamical quantity f then reads

$$\frac{df}{d\tau} = \{f, H_{2\mathrm{ph}}\} \equiv -i\sum_{s=0,2,\mathrm{L}}\left(\frac{\partial f}{\partial b_s}\frac{\partial H_{2\mathrm{ph}}}{\partial b_s^*} - \frac{\partial f}{\partial b_s^*}\frac{\partial H_{2\mathrm{ph}}}{\partial b_s}\right), \tag{C2}$$

where we have defined the Poisson brackets for the complex amplitudes b_0, b_2, and $b_\mathrm{L} \equiv a_\mathrm{L}$ of three harmonic oscillators. This semiclassical approximation neglects contributions that are responsible for spontaneous emission and thus we deduce that our approximation works for a seeded FEL, but breaks down for self-amplified spontaneous emission (SASE).

For the time evolution of the photon number $n \equiv |a_\mathrm{L}|^2$, we obtain the second-order differential equation

$$\ddot{n} = 4\varepsilon^4\left[4nN_0N_2 + n_0^2(N_0 - N_2)\right] \tag{C3}$$

with $N_s \equiv |b_s|^2$. We assume that the two constants of motion, $\hat{A}$ and $\hat{B}$, are described by their initial expectations values, that is $A = N$ and $B = 2N + n_0$, respectively. With the help of these relations we eliminate N_0 and N_2 in Eq. (C3) and obtain a closed equation for n. After integrating twice with respect to time τ, we observe

$$2\alpha_N^2\tau = \int_{n_0/N}^{n/N}\frac{d\xi}{\xi\sqrt{\left(\xi-\frac{n_0}{N}\right)\left(2+\frac{n_0}{N}-\xi\right)}}, \tag{C4}$$

which can be solved analytically. Finally, we arrive at the expression in Eq. (9) for the evolution of the photon number $n = n(L)$, where we have introduced the interaction length L via the relation $\alpha_N\tau = L/(2L_g)$ [13].

2. Numerical simulation

To find a numerical solution for the dynamics dictated by the effective Hamiltonian for $p = q$, we first consider the contribution corresponding to the two-photon Dicke Hamiltonian $\hat{H}_{2\mathrm{ph}}$. Similarly to Ref. [10], we notice the analogy of the jump operators to angular momentum, that is $\hat{J}_+ = \hat{\Upsilon}_{0,2}$, $\hat{J}_- = \hat{\Upsilon}_{2,0}$, and $\hat{J}_z = (\hat{\Upsilon}_{0,0} - \hat{\Upsilon}_{2,2})/2$. By applying the ladder operators $\hat{J}_\pm$ on the state $|r, m\rangle$, we obtain the relation [40]

$$\hat{J}_\pm|r, m\rangle = \sqrt{(r \pm m + 1)(r \mp m)}\,|r, m \pm 1\rangle, \tag{C5}$$

where r and m correspond to the quantum numbers of total angular momentum and its z component, respectively.

In this description, the initial state of the electrons is given by $|N/2, N/2\rangle = |p, p, ..., p\rangle$. In this case, only superpositions of the following states

$$|\mu\rangle \equiv |n_0 + 2\mu\rangle\,|N/2, N/2 - \mu\rangle \tag{C6}$$

can be populated by $\hat{H}_{2\mathrm{ph}}$, if we assume that the laser field starts from a Fock state with n_0 photons [36]. The quantum number μ runs from 0 to N, due to $-r \leqslant m \leqslant r$ with $r = N/2$.

We note that the second contribution $\hat{\Delta} \equiv \hat{H}_{\mathrm{eff}} - \hat{H}_{2\mathrm{ph}}$ to the effective Hamiltonian (compare to Table I) includes operators outside this angular momentum algebra. To proceed, we write the electron part of the state in Eq. (C6) in the form

$$|N/2, N/2-\mu\rangle = \frac{1}{\sqrt{\mu!}}\sqrt{\frac{(N-\mu)!}{N!}}\,\hat{J}_-^{\mu}\,|N/2, N/2\rangle \tag{C7}$$

which follows from Eq. (C5). With the help of this relation and the commutation relation for the jump operators in Eq. (A2) we calculate the action of $\hat{\Delta}$ on the state $|\mu\rangle$ and find that it is an eigenstate of $\hat{\Delta}$. Hence, we still can rely on the formalism for $\hat{H}_{2\mathrm{ph}}$ for the full effective Hamiltonian since $\hat{\Delta}$ reproduces only states in the form of Eq. (C6).

After expanding the quantum state $|\Psi\rangle$ of the total system in terms of the basis states $|\mu\rangle$, and applying the Schrödinger equation with the effective Hamiltonian for an initial momentum p, we finally obtain the equation of motion

$$i\frac{dc_\mu(L)}{d(L/L_g)} = a_p(\mu)c_{\mu-1}(L) + a(\mu+1)c_{\mu+1}(L) + d_p(\mu)c_\mu(L) \tag{C8}$$

for the expansion coefficients $c_\mu \equiv \langle\mu|\Psi\rangle$. For $p = q$, the off-diagonal terms

$$a_q(\mu) \equiv \frac{\alpha_N}{2}\sqrt{(n_0+2\mu-1)(n_0+2\mu)}\sqrt{\frac{\mu}{N}}\sqrt{1-\frac{\mu-1}{N}} \tag{C9a}$$

emerge from the two-photon Dicke Hamiltonian $\hat{H}_{2\mathrm{ph}}$ and

$$d_q(\mu) = \alpha_N\left[\frac{2}{3}\mu\left(1-\frac{1}{N}\right)+\frac{1}{3}n_0+\frac{1}{2}\right] \tag{C9b}$$

represents the additional diagonal contributions arising from $\hat{\Delta}$. Similarly to Appendix C 1, we transformed from τ to L. The probability amplitudes c_μ contain all information of the quantum state of the system and after computing them numerically by diagonalizing a $(N+1)\times(N+1)$ tri-diagonal matrix we are able to evaluate any expectation value.

Analogously, we find for the resonance $p = q/2$ a dynamical equation of the same form as Eq. (C8) using the corresponding effective Hamiltonian from Table I up to third order. In this case, the ladder operators of angular momentum are given by $\hat{\Upsilon}_{1,0}$ and $\hat{\Upsilon}_{0,1}$. We obtain the expressions

$$a_{q/2}(\mu) \equiv \frac{1}{2}\left[1-\frac{\alpha_N^2}{8}\left(1+2\frac{n_0+1}{N}\right)\right]\sqrt{\mu(n_0+\mu)}\sqrt{1-\frac{\mu-1}{N}} \tag{C10a}$$

and

$$d_{q/2}(\mu) \equiv -\frac{\alpha_N}{4}\left[n_0+\mu\left(1+\frac{1}{N}\right)\right] \tag{C10b}$$

for the off-diagonal and diagonal terms in the differential equation.

[1] C. B. Schroeder, C. Pellegrini, and P. Chen, Quantum effects in high-gain free-electron lasers, Phys. Rev. E **64**, 056502 (2001).

[2] N. Piovella, M. M. Cola, L. Volpe, A. Schiavi, and R. Bonifacio, Three-Dimensional Wigner-Function Description of the Quantum Free-Electron Laser, Phys. Rev. Lett. **100**, 044801 (2008).

[3] R. Bonifacio, H. Fares, M. Ferrario, B. W. J. McNeil, and G. R. M. Robb, Design of sub-Angstrom compact free-electron laser source, Opt. Commun. **382**, 58 (2017).

[4] A. Serbeto, L. F. Monteiro, K. H. Tsui, and J. T. Mendonça, Quantum plasma fluid model for high-gain free-electron lasers, Plasma Phys. Control. Fusion **51**, 124024 (2009).

[5] P. Kling, E. Giese, R. Endrich, P. Preiss, R. Sauerbrey, and W. P. Schleich, What defines the quantum regime of the free-electron laser? New J. Phys. **17**, 123019 (2015).

[6] M. S. Brown, J. R. Henderson, L. T. Campbell, and B. W. J. McNeil, An extended model of the quantum free-electron laser, Opt. Express **25**, 33429 (2017).

[7] P. M. Anisimov, Quantum theory for 1D x-ray free electron laser, J. Mod. Opt. **65**, 1370 (2018).

[8] B. H. Schaap, S. Schouwenaars, and O. J. Luiten, A Raman quantum free-electron laser model, Phys. Plasmas **29**, 113302 (2022).

[9] R. Bonifacio, N. Piovella, G. R. M. Robb, and A. Schiavi, Quantum regime of free electron lasers starting from noise, Phys. Rev. ST Accel. Beams **9**, 090701 (2006).

[10] P. Kling, E. Giese, C. M. Carmesin, R. Sauerbrey, and W. P. Schleich, High-gain quantum free-electron laser: Long-time dynamics and requirements, Phys. Rev. Res. **3**, 033232 (2021).

[11] A. Debus, K. Steiniger, P. Kling, C. M. Carmesin, and R. Sauerbrey, Realizing quantum free-electron lasers: A critical analysis of experimental challenges and theoretical limits, Phys. Scr. **94**, 074001 (2019).

[12] E. A. Seddon, J. A. Clarke, D. J. Dunning, C. Masciovecchio, C. J. Milne, F. Parmigiani, D. Rugg, J. C. H. Spence, N. R. Thompson, K. Ueda, S. M. Vinko, J. S. Wark, and W. Wurth, Short-wavelength free-electron laser sources and science: A review, Rep. Prog. Phys. **80**, 115901 (2017).

[13] P. Kling, E. Giese, C. M. Carmesin, R. Sauerbrey, and W. P. Schleich, High-gain quantum free-electron laser: Emergence and exponential gain, Phys. Rev. A **99**, 053823 (2019).

[14] R. Bonifacio and H. Fares, A fully quantum theory of high-gain free-electron laser, Europhys. Lett. **115**, 34004 (2016).

[15] P. Bosco, W. Colson, and R. Freedman, Quantum/classical mode evolution in free electron laser oscillators, IEEE J. Quantum Electron. **19**, 272 (1983).

[16] A. Bambini and A. Renieri, The free electron laser: A single-particle classical model, Lett. Nuovo Cimento **21**, 399 (1978). A. Bambini, A. Renieri, and S. Stenholm, Classical theory of the free-electron laser in a moving frame, Phys. Rev. A **19**, 2013 (1979).

[17] W. Becker, M. O. Scully, and M. S. Zubairy, Generation of Squeezed Coherent States via a Free-Electron Laser, Phys. Rev. Lett. **48**, 475 (1982).

[18] K. Steiniger, M. Bussmann, R. Pausch, T. Cowan, A. Irman, A. Jochmann, R. Sauerbrey, U. Schramm, and A. Debus, Optical free-electron lasers with traveling-wave Thomson-scattering, J. Phys. B: At. Mol. Opt. Phys. **47**, 234011 (2014).

[19] G. R. M. Robb and R. Bonifacio, Coherent and spontaneous emission in the quantum free electron laser, Phys. Plasmas **19**, 073101 (2012).

[20] W. H. Louisell, J. F. Lam, and D. A. Copeland, Effect of space charge on free-electron-laser gain, Phys. Rev. A **18**, 655 (1978).

[21] P. Sprangle and R. A. Smith, Theory of free-electron lasers, Phys. Rev. A **21**, 293 (1980).

[22] N. N. Bogoliubov and Y. A. Mitropolsky, *Asymptotic Methods in the Theory of Non-Linear Oscillations* (Hindustan Publishing Corporation, Delhi, 1961).

[23] L. L. Buishvili, E. B. Volzhan, and M. G. Menabde, Higher approximations in the theory of the average Hamiltonian, Teor. Mat. Fiz. **46**, 166 (1981).

[24] P. Schmüser, M. Dohlus, and J. Rossbach, *Ultraviolet and Soft X-Ray Free-Electron Lasers* (Springer, Heidelberg, 2008).

[25] P. Kling, Theory of the free-electron laser: From classical to quantum, Ph.D. thesis, Universität Ulm, 2018, http://dx.doi.org/10.18725/OPARU-5238.

[26] C. M. Carmesin, P. Kling, E. Giese, R. Sauerbrey, and W. P. Schleich, Quantum and classical phase-space dynamics of a free-electron laser, Phys. Rev. Res. **2**, 023027 (2020).

[27] N. Piovella and R. Bonifacio, Inhomogeneous effects in the quantum free electron laser, Nucl. Instrum. & Methods A **560**, 240 (2006).

[28] S. Kunze, S. Dürr, and G. Rempe, Bragg scattering of slow atoms from a standing light wave, Europhys. Lett. **34**, 343 (1996).

[29] H. Ahlers, H. Müntinga, A. Wenzlawski, M. Krutzik, G. Tackmann, S. Abend, N. Gaaloul, E. Giese, A. Roura, R. Kuhl, C. Lämmerzahl, A. Peters, P. Windpassinger, K. Sengstock, W. P. Schleich, W. Ertmer, and E. M. Rasel, Double Bragg Interferometry, Phys. Rev. Lett. **116**, 173601 (2016).

[30] R. Bonifacio, F. Casagrande, and L. De Salvo Souza, Collective variable description of a free-electron laser, Phys. Rev. A **33**, 2836(R) (1986).

[31] R. H. Dicke, Coherence in spontaneous radiation processes, Phys. Rev. **93**, 99 (1954).

[32] P. F. Byrd and M. D. Friedman, *Handbook of Elliptic Integrals for Engineers and Scientists* (Springer, Berlin, 1971).

[33] G. Compagno, J. S. Peng, and F. Persico, Squeezing in a two-photon Dicke hamiltonian, Opt. Commun. **57**, 415 (1986).

[34] C. C. Gerry and J. B. Togeas, Squeezing and photon antibunching from a two-photon dicke model, Opt. Commun. **69**, 263 (1989).

[35] S. Kumar and C. L. Mehta, Theory of the interaction of a single-mode resonant radiation field with N two-level atoms, Phys. Rev. A **21**, 1573 (1980).

[36] D. F. Walls and R. Barakat, Quantum-mechanical amplification and frequency conversion with a trilinear Hamiltonian, Phys. Rev. A **1**, 446 (1970).

[37] R. Bonifacio, Quantum SASE FEL with laser wiggler, Nucl. Instrum. & Methods A **546**, 634 (2005).

[38] A. H. Nayfeh, *Perturbation Methods* (Wiley, New York, 1973).

[39] J. Schwinger, On angular momentum, Tech. Rep. (United States Atomic Energy Comission, 1952).

[40] C. Cohen-Tannoudji, B. Diu, and F. Laloë, *Quantum Mechanics* (Wiley, Singapore, 1977), Vol. 1.